Dynamic regimes in MgB_2 probed by swept frequency microwave measurements

S. Sarti and C. Amabile
Dipartimento di Fisica, Università "La Sapienza," P.le Aldo Moro 2, 00185 Roma, Italy

E. Silva
Dipartimento di Fisica "E.Amaldi" and INFM-Coherentia, Università "Roma Tre," Via della Vasca Navale 84, 00146 Roma, Italy

M. Giura and R. Fastampa
Dipartimento di Fisica and INFM-Coherentia, Università "La Sapienza," P.le Aldo Moro 2, 00185 Roma, Italy

C. Ferdeghini, V. Ferrando, and C. Tarantini
INFM—LAMIA, Dipartimento di Fisica, Università di Genova, Via Dodecanneso 33, 16146 Genova Italy
(Received 9 February 2005; revised manuscript received 12 April 2005; published 27 July 2005)

We report swept frequency measurements (2–20 GHz) of the microwave resistivity in MgB_2, in the presence of a static magnetic field. Through these data, we experimentally determine the region of the $\{H,T\}$ plane in which the π band does not significantly contribute to the superfluid density. Within that region, we show that data can be interpreted through standard models for vortex motion and quasiparticle resistivity. We obtain the temperature-dependent σ band superfluid density and the upper critical field. We find excellent agreement between the dc and microwave estimates of the upper critical field. The temperature-dependent superfluid density agrees with a BCS calculation based on independently obtained data for the large gap. We also measure and discuss the vortex characteristic frequency due to pinning effects.

DOI: 10.1103/PhysRevB.72.024542 PACS number(s): 74.70.Ad, 74.20.De, 74.25.Nf, 74.25.Op

I. INTRODUCTION

The complexity of the $\{H,T\}$ diagram of magnesium diboride (MgB_2) has stimulated in the last years a large amount of papers, related to the study of the various characteristic magnetic fields of the material.[1] The presence of two electronic bands (π and σ bands) is in this view a fundamental challenge, and a number of techniques have been used to get information on the superconducting parameters of both these bands and of the material altogether.[2] Among other studies, the electromagnetic response of MgB_2 at microwave frequencies has attracted the interest of researchers,[3] due to the large number of interesting physical parameters that can be detected through the microwave measurements. A particular research topic is the response in presence of an applied static magnetic field. When analyzing the microwave response in a magnetic field, most of the reported analysis relyies on the assumption of validity of the two-fluid model and more or less standard dynamics for vortices.[4,5] In the case of MgB_2, however, one has to take into account that the presence of two coexisting superfluids (coming from the σ and π bands) makes the standard two-fluid model not necessarily adequate for this material. In particular, the observed temperature dependence of the zero field penetration depth cannot be described by standard two-fluid expressions.[3]

Further, vortices are predicted to have more complex structure than standard ones,[6] suggesting that the standard models for the flux dynamics could fail when applied to MgB_2. Finally, even in standard superconductors, the two-fluid model is not reliable close to the transition to the normal state where different phenomena (fluctuations, coherence effects) are expected to occur.[7] The description of the mixed state of MgB_2 in terms of two fluid models and standard vortices might then be inadequate in large regions of the $\{H,T\}$ phase diagram (see Fig. 1).

A number of experimental works have shown, on the other hand, that a relatively sharp crossover occurs, within the mixed state, at low field. Scanning tunnel experiments[8] showed that the superconductivity coming from the π band is strongly suppressed by applying a field as low as 0.5 T. Similar results have been observed by point contact spectroscopy.[9] It was also shown[10] that the vortex lattice undergoes a spatial rotation when the magnetic field becomes of order 0.5–1 T, indicating that relevant changes on the vortex interactions among themselves and with the underly-

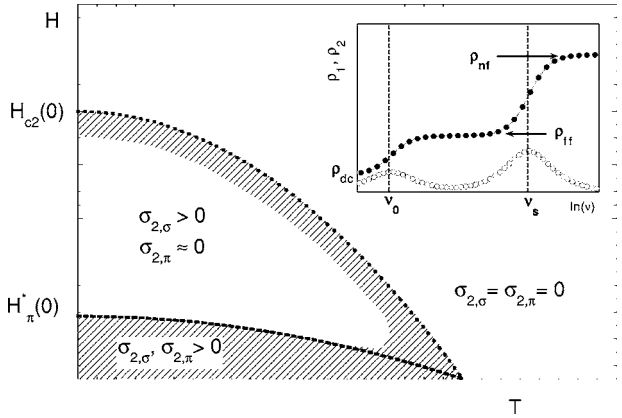

FIG. 1. Main panel: regions of the $\{H,T\}$ phase diagram where the two-fluid model could fail (shaded regions, see text) and expected values for the superfluid conductivity σ_2 of the two bands. Inset: general shape of the curves $\rho_1(\nu)$ (filled circles) and $\rho_2(\nu)$ (open circles) according to Eq. (2).

ing crystal lattice occur in that field range. All these results suggest that above a relatively low field H^* the superfluid fraction of the π band is strongly suppressed, and vortices change their nature from the complex, composite structure predicted at low fields to a more standard, "single-band-like" structure.

In this paper, we present a large set of measurements of the microwave complex resistivity $\tilde{\rho}=\rho_1+i\rho_2$, as a function of temperature T, magnetic field H and frequency ν. These measurements are performed on a MgB_2 film through a Corbino disk technique, which allows us to have information on both the real and the imaginary part of the resistivity over a continuous, wide band (2–20 GHz) spectrum. We will show that through these data it is possible to experimentally define a temperature dependent magnetic field H_1, which can be identified with the field H^*. Further, we will show that the microwave response above H^* can be described by a generalized form of the conventional one-band model for the response of vortices, superfluid and normal fluid, in which the "normal fluid" is given by the normal part of the σ band plus the π band, the "superfluid" is given by the superconducting fluid of the σ band, and vortices can be described as standard ones. In the following, we will refer to this model as a "generalized two-fluid/vortex" (GTFV) model. We obtain the physical parameters which characterize, within this simple model, the normal fluid, the superfluid, and the vortices. We find for the first time a good, quantitative agreement between the parameters obtained through microwave data and those obtained through independent measurements.

The paper is organized as follows: in Sec. II, we recall the main results of the model that we use for the description of the microwave resistivity data, and we discuss its applicability to the case of MgB_2. In Sec. III we summarize the experimental setup used and sample characteristics. In Sec. IV we describe and discuss the experimental results. Brief conclusions are reported in Sec. V.

II. THEORY

Within the limit of validity of the two-fluid model, a very general expression for the surface impedance of a semi-infinite superconductor in the mixed state is[11]

$$Z_s(B,T)=\mathrm{i}\omega\mu_0\tilde{\lambda}=\mathrm{i}\omega\mu_0\left(\frac{\lambda^2(B,T)-(\mathrm{i}/2)\tilde{\delta}_v^2(B,T,\omega)}{1+2\mathrm{i}\lambda^2(B,T)/\delta_{nf}^2(B,T,\omega)}\right)^{1/2}, \tag{1}$$

where $\lambda(B,T)=\lambda_0/\sqrt{n_s(B,T)}$ is the London penetration depth, $n_s(B,T)$ is the superfluid fraction, $\delta_{nf}(B,T,\omega)=(2\rho_{nf}/\mu_0\omega)^{1/2}$ is the normal fluid skin depth, $\rho_{nf}(B,T)=1/\sigma_{nf}=1/[n_n(B,T)\sigma_n]$ is the (real) resistivity due to quasiparticles,[12] $n_n(B,T)=1-n_s(B,T)$ is the normal fluid fraction, $\sigma_n=1/\rho_n$ is the normal state conductivity, and $\tilde{\delta}_v^2(B,T,\omega)$ is the complex penetration depth arising from vortex motion. The surface impedance Z_s is related to the complex microwave resistivity of the superconductor $\tilde{\rho}$ through the standard relation $Z_s=(\mathrm{i}\omega\mu_0\tilde{\rho})^{1/2}$. One then gets $\tilde{\rho}=\rho_1+\mathrm{i}\rho_2=\mathrm{i}\omega\mu_0\tilde{\lambda}^2$ and, after some algebra

$$\frac{\rho_1}{\rho_n}=\frac{1}{1+(\nu/\nu_s)^2}\left(r_1(\nu,B,T)+\frac{\nu}{\nu_s}r_2(\nu,B,T)\right),$$

$$\frac{\rho_2}{\rho_n}=\frac{1}{1+(\nu/\nu_s)^2}\left(r_2(\nu,B,T)-\frac{\nu}{\nu_s}r_1(\nu,B,T)\right), \tag{2}$$

where $r_1=\mathrm{Re}[\rho_v]/\rho_n$, $r_2=\mathrm{Im}[\rho_v]/\rho_n+(\rho_{nf}/\rho_n)(\nu/\nu_s)$, $\rho_v=\mu_0\omega\tilde{\delta}_v^2/2$ is the complex resistivity due to the motion of vortices, and $\nu_s(B,T)=[\rho_{nf}(B,T)]/[2\pi\mu_0\lambda^2(B,T)]$. It is easy to verify that with this definition of ν_s, one has $\nu/\nu_s=(\lambda/\delta_{nf})^2$, so that ν_s is the frequency above which δ_{nf} becomes shorter than λ. Equations (2) contains in a self-consistent way both the quasiparticle contribution (through ν_s and ρ_{nf}) and the motion of vortices (through ρ_v). The model is founded on the interaction between charge carriers and a system of magnetic vortices moving under the influence of rf currents and pinning phenomena. Charge carriers are thought as bearing superconducting currents, represented by a single superfluid fraction $n_s(B,T)$, which gives rise to an imaginary conductivity, and normal currents, represented by a normal, real conductivity σ_{nf}. It is not clear at present whether the model can be extended to include the interaction of different supercurrents, coming from σ and π superfluids, with composite vortices, as predicted in two-band superconductors.[6] However, in the region of the $\{H,T\}$ phase diagram above H^*, we expect that the GTFV model [which is founded on the same hypotheses from which are obtained Eqs. (2)] is an adequate description of the superconductor. We then expect that Eqs. (2) can be safely used above H^*.

Equations (2) are equivalent to expressions widely used for the microwave resistivity of a superconductor in the mixed state when some further approximations are satisfied. In particular, they reduce to the conventional Gittleman-Rosenblum expressions for the resistivity[13] in the limit $\nu/\nu_s \ll 1$ (that is, when the quasiparticle response can be neglected) and using the standard expressions for the vortex resistivity ρ_v. However, this limit is oversimplified with respect to the more general case of a superconductor in a magnetic field: the limit $\nu/\nu_s \ll 1$ is not always satisfied, while different expressions have been proposed for the behavior of ρ_v as a function of frequency, magnetic field, and temperature, depending on the specific features of the potential seen by vortices during their motion (pinning potential, surface barriers, etc.).[14] Whichever is the model for ρ_v, there are however some general features that can be stated on the motion of vortices in different dynamical regimes: at rather low frequencies, vortices are induced to move over large distances, thus probing the pinning profile. In the presence of strong enough pinning or interactions with other vortices, the mobility of vortices will then result lower than the free flow value, so that $\mathrm{Re}[\rho_v]<\rho_{ff}=\Phi_0 B/\eta$ and in general $\mathrm{Im}[\rho_v] \propto \nu > 0$. With increasing frequency, and above a vortex characteristic frequency ν_0, the oscillation amplitude becomes so small that the pinning potential is nearly ineffective, resulting in a purely dissipative vortex motion with $\mathrm{Re}[\rho_v]=\rho_{ff}$ and $\mathrm{Im}[\rho_v]=0$. The real part of ρ_v is then expected to increase from the dc value to the free flow value ρ_{ff} with increasing frequency. More, in the frequency range in which

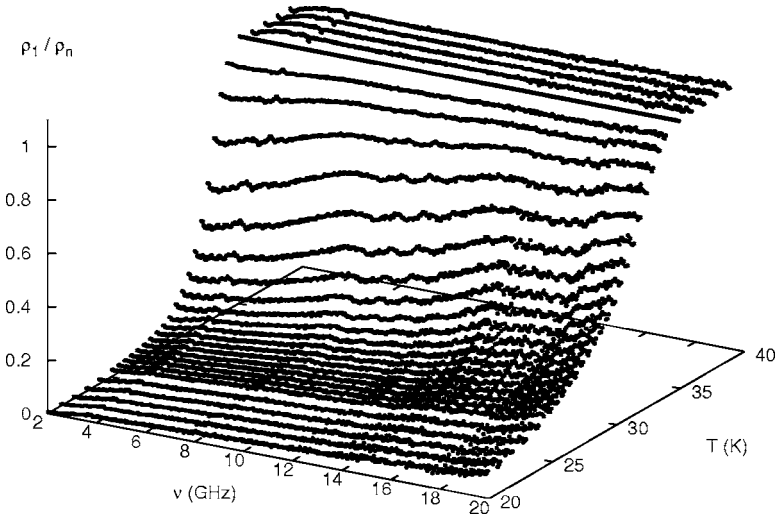

FIG. 2. The frequency and temperature dependence of the real part of the resistivity with no applied magnetic field, normalized at 36 K. Isothermal curves are plotted.

the crossover takes place, $\mathrm{Im}[\rho_v]$ presents a maximum around the characteristic frequency ν_0, being essentially zero both at zero frequency and at large frequencies. Interestingly, Eqs. (2) present the same features around the second characteristic frequency ν_s (an increase, followed by a plateau, in ρ_1 and a peak in ρ_2 for $\nu \simeq \nu_s$) so that any variation of the real part of $\tilde{\rho}$ as a function of frequency is followed by a corresponding variation of the imaginary part, in the same frequency range. Schematic shapes of the curves ρ_1 and ρ_2 as obtained from Eqs. (2) are reported in the inset of Fig. 1 using for ρ_v the frequency dependence obtained in Ref. 11 (the detailed shapes of ρ_1 and ρ_2 might be different around ν_0 if one considers different models for the vortex dynamics). We stress that, since both ν_s and ν_0 depend on T and H, the section of the curve explored by measurements performed at fixed frequency (or, as in our case, at fixed frequency interval) might change with T and H, making the extraction of physical parameters extremely difficult. In particular, should the frequency ν_0 change abruptly as a function of field, any measurement at fixed frequency (with $\nu \simeq \nu_0$) would hardly give any information on the various parameters involved in the expressions of the resistivity, unless very specific models for the vortex dynamics are invoked.

III. EXPERIMENTAL SETUP AND SAMPLES

Measurements are performed on a square (l=5 mm), thin (d=100 nm) MgB_2 film, grown by pulsed laser deposition with a two-step technique on c-cut sapphire substrate. Details on the sample preparation can be found in Ref. 15. The sample is oriented both along the c axis (the FWHM measured from the rocking curve on this particular sample was 1.2°) and within the plane, with $\rho(40\ \mathrm{K})=5\ \mu\Omega\ \mathrm{cm}^{-1}$. Estimates of the critical fields parallel to the planes ($H^{dc}_{c2,\parallel}$) and to the c axis ($H^{dc}_{c2,\perp}$), and of the critical temperature T^{dc}_c=36 K, were obtained by resistivity measurements in magnetic field up to 9 T, using standard four-probe technique and a criterion of the 90% of the normal state resistance. Through this definition, one gets an approximately linear behavior of $H^{dc}_{c2,\perp}(T)$ down to 4.2 K (see Fig. 5) and an anisotropy ratio $\gamma = H^{dc}_{c2,\parallel}/H^{dc}_{c2,\perp} \simeq 3$, decreasing with increasing temperature.[16] Measurements in the microwave range are obtained through a Corbino disk geometry: a swept frequency microwave radiation is generated by a vector network analyzer (VNA) and guided to the sample under study through a coaxial cable. The sample, placed inside the cryomagnetic apparatus, short-circuits the coaxial cable. Measuring the reflection coefficient Γ_m of the whole system (cable and sample) through the VNA, we then obtain the effective impedance of the sample as a function of frequency, magnetic field (up to 12 T, always perpendicular to the film plane) and temperature. To this end, a custom procedure is used to extract from Γ_m the part due to the sample only, that is the reflection coefficient at the sample surface Γ_0 which is related to the effective surface impedance Z_{eff} of the sample by the standard relation

$$\Gamma_0 = \frac{Z_{eff} - Z_0}{Z_{eff} + Z_0},$$

where Z_0 is the impedance of the cable. Due to the small thickness of the sample, the thin film approximation holds[17] and one has $Z_{eff}=\tilde{\rho}/d$. Thus, contrary to the case of measurements on crystalline or bulk samples, in the case of thin films the real and imaginary parts of Z_{eff} directly give the values of ρ_1 and ρ_2. Details of the experimental procedure and tests of the correctness of the approximations involved can be found in Ref. 18. Corbino disk measurements are performed in a static magnetic field up to 12 T applied parallel to the c axis. Using this technique, we determine the complex resistivity $\tilde{\rho}$ of the sample in a one decade wide (2–20 GHz) frequency range, over the whole $\{H,T\}$ superconducting phase diagram.

In Fig. 2 we report the real part of the complex resistivity $\tilde{\rho}$, for H=0, as a function of temperature and frequency. As can be seen, the resistive transition is reasonably sharp at low frequency (ν=2 GHz), while it widens at larger ν. This feature is common to other MgB_2 films of the same batch, while it is not observed in $YBa_2Cu_3O_{7-\delta}$ samples,[18] indicating that it is more likely due to some characteristic of MgB_2 rather than to some feature of the technique used.

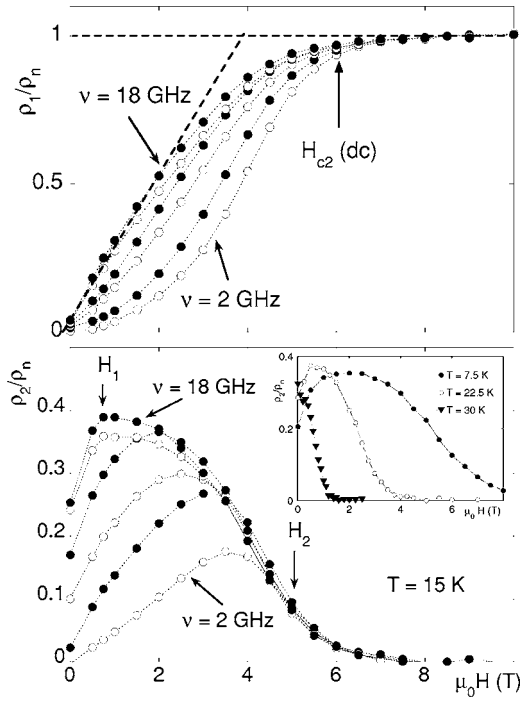

FIG. 3. Upper panel: ρ_1/ρ_n at various frequencies (ν =2,5,6,12,15,18 GHz), at T=15 K as a function of field. The extrapolated value for H_{c2} (see text) results to be much lower than the upper critical field obtained through *dc* data. Lower panel, main panel: ρ_2/ρ_n at the same frequencies and temperature, as a function of field. The arrows mark the two characteristic fields H_1 and H_2 (see text). In the inset, ρ_2/ρ_n at different temperatures (ν =17.5 GHz) showing the evolution of the field H_1 as a function of T.

IV. EXPERIMENTAL RESULTS AND DISCUSSION

As a first step, we present the measured data as a function of magnetic field, at fixed temperature and different frequencies. In Fig. 3 we report the measured ρ_1 (upper panel) and ρ_2 (lower panel), normalized to the normal state resistivity ρ_n, as a function of field for T=15 K. Similar results are obtained at all temperatures.[19] We first try to examine our results within the somehow conventional view of the vortex motion as the unique source of the magnetic response. In other words, we try to analyze the data by assuming the validity of the GTFV model for all fields and temperatures, neglecting also the quasiparticle contribution ($\nu/\nu_s \ll 1$). We first focus our attention on ρ_1. The observed behavior could be, in principle, explained in terms of vortex motion only: as expected from the general considerations mentioned above, the real resistivity grows, at fixed field and temperature, as a function of frequency, reflecting the lower and lower efficacy of the pinning phenomena as the frequency is increased. More, as the frequency is increased ($\nu > 12$ GHz), the observed frequency dependence of ρ_1 becomes smaller and smaller, while ρ_1 becomes linear as a function of field, as it would be expected for the flux flow limit predicted at high frequency. However, in this framework the upper critical field should be identified as the point where $\rho_{ff}/\rho_n = H/H_{c2}$ (obtained as the extrapolation of the linear slope at small fields) is equal to one. The critical field obtained in this way would result much lower than the H_{c2}^{dc} measured on the same sample through dc measurements (see figure). Further, the linearity of ρ vs. H is restricted to rather low fields ($H < 3$ T), that is just to about $H_{c2}^{dc}/2$. If, on the other hand, one assumes $\rho_{ff} = \rho_n H/H_{c2}$ at all fields, this would result in an apparently field-dependent upper critical field. An analysis of this kind has been performed in Ref. 20.

These puzzling results find a counterpart in the behavior as a function of field of ρ_2/ρ_n (see Fig. 3, lower panel). Two main features are clearly evident: the first one is observed at low fields ($H < H_1$, operatively defined in Fig. 3; see also the next subsection) and high frequencies (in this case, $\nu > 15$ GHz), where the observed ρ_2/ρ_n increases abruptly at low fields, then smoothly decreases as the field is further increased. The second one is seen at high fields ($H > H_2$, operatively defined in Fig. 3; see also the next subsection) where ρ_2/ρ_n, though clearly nonzero, is almost constant as a function of frequency over a variation of one order of magnitude for ν. Both these features are difficult to be interpreted in terms of vortex motion: in fact, a rapid growth of ρ_2 at high frequency can be explained only assuming that the characteristic frequency for the vortex motion ν_0 is close to 15 GHz and strongly field dependent. However, measurements of ρ_1 in the same field range (see the upper panel of the same figure) seem to indicate that the flux flow limit is reached at the same frequencies, that is, ν_0 is sufficiently lower than 15 GHz. On the other hand, a constant but not zero value of ρ_2 is never predicted over a one decade wide range of frequencies, so that the dynamics of the superconductor at high fields, as resulting from our data, can hardly be described in terms of conventional models. We note that the raw experimental data here presented, if sampled at a single frequency, are in substantial agreement with previous single frequency measurements[4] obtained through the resonant cavity technique. In that case the rounding of the ρ_1 vs. H curves was interpreted as a signature of large effects of fluctuations across H_{c2}. Discrepancies still took place, in particular the values of H_{c2} obtained through a fluctuational scaling procedure were found to be still lower than the values found in literature. We stress, however, that swept-frequency measurements on one side highlight much deeper inconsistencies with the identification of the response with vortex motion alone, while on the other hand reveal a clearly richer physics of the vortex state in MgB_2. As we will see in the following, the frequency-dependent measurements and a proper analysis of these data lead to a consistent interpretation of the field, temperature, and frequency dependence of the microwave response in the intermediate field region. In particular, we will see that it is essential to include the temperature and field dependence of the quasiparticle contribution.

A. Determination of crossover fields

As a first step, we analyze the low field data. We focus the attention on the high-frequency data, since they are much less affected by the severe complications arising from pinning as can be inferred by the little frequency dependence of

ρ_1 at these frequencies. As previously discussed, a steep increase of ρ_2 vs. H is observed, up to a temperature-dependent field H_1. The temperature evolution of this feature is presented in the inset of the same figure. The temperature dependence of the field H_1 is regular, and it is presented in Fig. 5. We now show that the field H_1 can be identified with the field H^* above which the superfluid contribution of the π band is expected to be negligible. To this end, we notice that, as discussed above, the ρ_1 data indicate that ν_0 is sufficiently lower than 15 GHz. As a consequence, at high frequency and low fields, if the GTFV model is applicable, one may take as a first approximation $r_1 \simeq \Phi_0 B/\eta\rho_n$ and $r_2 \simeq (\rho_{nf}/\rho_n)\nu/\nu_s$, so that one may write

$$\frac{\rho_2}{\rho_n} = \frac{\nu/\nu_s}{1+(\nu/\nu_s)^2}\left(\frac{\rho_{nf}}{\rho_n} - \frac{\Phi_0}{\eta\rho_n}B\right) \simeq \frac{2\pi\nu\mu_0\lambda^2}{\rho_n}\left(\frac{\rho_{nf}}{\rho_n} - \frac{\Phi_0}{\eta\rho_n}B\right), \tag{3}$$

where for the last approximate equality we used the definition of ν_s and the fact that at low enough fields and temperatures one expects $(\nu/\nu_s)^2 \ll 1$. In a single-band superconductor, at low fields the decrease of the term within square brackets overcomes the increase of λ, leading to a decreasing ρ_2 vs. B. The same behavior is expected in MgB_2 above H^*, since in that case also there is only one field scale (H/H_{c2}) for both the superfluid density and the free vortex motion. It is then reasonable to identify H_1 with H^*, the traditional behavior observed only above H_1. This identification is further confirmed by the behavior as a function of T of the field H_1 (see Fig. 3, inset of the lower panel, and Fig. 5): as expected, H_1 decreases as a function of T, until at temperatures close to T_c the peak for $\rho_2(H)$ disappears, and H_1 cannot be defined any longer. Further, the numerical values of H^* defined in this way are in good agreement with independent estimates of the same characteristic field.[8–10,21] The rapid growth of ρ_2 for $H < H^*$ can be qualitativley explained as follows: being the vortex motion simplified to the flux-flow limit (this is clearly true only at high frequencies) below H^* the field scale for the flux motion is given again by the upper critical field, while λ is expected to steeply increase as the conductance of the π-band superfluid becomes negligible, that is between $H=0$ and the characteristic field H^*. The behavior of ρ_2 at low fields and high frequency can thus be understood as a signature of the rapid growth of λ for $H \to H^*$, followed by the standard decrease as a function of field when the material, at higher fields, becomes comparable to a single-band superconductor. We note that at lower frequencies the variation of ρ_2 as a function of field is by far more complex, involving also the variation of ν_0 with H. Since it has been shown[10] that the vortex lattice changes its orientation across H^*, it is reasonable to assume that also ν_0 (related to the pinning strength) might abruptly change across H^*, so that the response at low field can be rather difficult to be described at lower frequencies. Again, the frequency-dependent data are a key factor for a correct identification of different dynamic regimes.

We now come to the high field data. As discussed previously, we find an almost frequency independent, nonzero ρ_2. This finding cannot be explained in terms of Eqs. (2), for any choice of the parameters involved. Other contributions are indeed expected to come into play as the normal state is approached, such as fluctuations or coherence effects, so that the failure of Eqs. (2) is not surprising at high enough fields. On the other hand, it is reasonable that these contributions do not come abruptly into play, rather their relevance grows continuously as H_{c2} is approached. We then interpret the experimentally defined H_2 as being representative of a smooth crossover line in the H-T plane above which the GTFV model is no longer able to catch the main features of the superconducting response: above H_2, other contributions are strong enough as to make impossible to safely apply Eqs. (2).

B. Determination of H_{c2} and n_s

According to the previous discussion, $H_1(T)$ and $H_2(T)$ represent the border lines of the region in the $\{H,T\}$ plane where the GTFV model could be applicable (see Fig. 1). This peculiar two-fluid is characterized by a superfluid fraction $n_s(B,T)$ which is related to the superfluid fraction of the σ band $n_{s,\sigma}(B,T)=N_{s,\sigma}/N_\sigma$ (that is, the superfluid volume density divided by the total volume density of electrons in the σ band) through the relation $n_s(B,T)=Kn_{s,\sigma}(B,T)$, with $K=N_\sigma/(N_\sigma+N_\pi)$, N_π being the volume density of electrons in the π band. The corresponding normal fluid resistivity is given by an appropriate combination of the resistivities of the normal fluid of the σ band $\rho_{nf,\sigma}$ and the normal resistivity of the π band (we neglect the small fraction of electrons of the π band that might still be superconducting above H^*). Within the same region, we assume that vortices are standard (single-band) vortices, whose equation of motion is the same as for traditional vortices. All these assumptions lead to the validity of Eqs. (2).

In order to reduce the number of free parameters, we make some general considerations on the T and H dependencies of the parameters ν_s and ρ_{nf} describing the superfluid and the quasiparticles. First, we notice that above H_1, most of the electrons of the π band are in the normal state. In this case, λ is determined by the σ band only, so that $\lambda^2(B,T)=\lambda_{0,\sigma}^2/n_{s,\sigma}(B,T)=K\lambda_{0,\sigma}^2/n_s(B,T)$, where $\lambda_{0,\sigma}$ is the zero temperature, zero field value of the σ band penetration depth and we have used the relation $(\lambda_{0,\sigma}/\lambda_\sigma(B,T))^2=n_{s,\sigma}(B,T)$. One then gets

$$\nu_s(B,T) = C\frac{\rho_{nf}(B,T)}{\rho_n}n_s(B,T) \tag{4}$$

(where $C=\rho_n/2\pi\mu_0 K\lambda_{0,\sigma}^2$), so that the magnetic field and temperature variations of ν_s are entirely determined by the ratio ρ_{nf}/ρ_n and by the variation as a function of T and B of n_s.

Second, since it has been shown[22] that the two bands interact very weakly with each other, the overall conductivity of the normal fraction of the generalized two fluid superconductor above H_1 can be written as $\sigma_{nf}=\sigma_{n,\pi}+[1-n_{s,\sigma}(B,T)]\sigma_{n,\sigma}$. Further, using the determination of the upper critical fields through dc measurements, it is possible to estimate the normal state resistivities of the two bands: using

the Gurevich model[23] and the measured temperature variation of the anisotropy factor γ between the in-plane and the out-of-plane upper critical fields, we conclude that in our sample the σ band is characterized by a lower diffusivity than the π band ($D_\sigma < D_\pi$)[15,24] with a ratio $\sigma_{n,\sigma}/\sigma_{n,\pi} \simeq 0.25$. Both the normal state resistivity $\rho_n = 1/(\sigma_{n,\pi} + \sigma_{n,\sigma})$ and, to a larger extent [due to the $1 - n_{s,\sigma}(B,T)$ prefactor for $\sigma_{n,\sigma}$], $\rho_{nf} = 1/\sigma_{nf}$ are then close to $\rho_{n,\pi} = 1/\sigma_{n,\pi}$. We then conclude that, to a good approximation, one may take $\rho_{nf}/\rho_n = 1$ in all the field and temperature region $H > H_1(T)$, and that the T and B variations of $\nu_s(B,T)$ are entirely determined by $n_s(B,T)$.

Finally, bearing in mind that we refer to the intermediate field and temperature region (above H^* and sufficiently below H_{c2}), we can reasonably take the field dependence of the superfluid fraction as given by the standard expression for a superconductor with a single, *s*-like gap,[3,25] given by

$$n_s(B,T) = n_{s0}(T)(1-b), \tag{5}$$

where $b = B/B_{c2}(T) \simeq H/H_{c2}(T)$ and $n_{s0}(T) = K n_{s,\sigma}(B=0,T)$ is the (extrapolated) zero field value of n_s. We stress that $n_{s0}(T)$ is not related in a simple way to the value that is obtained through experiments that measure the superfluid density at $B=0$, being in that case $n_s^{meas}(B=0,T) = n_{s,\sigma}(B=0,T) + n_{s,\pi}(B=0,T)$.

Once the general frame has been defined, we use the resistivity data to extract the physical parameters defining the superfluid state. According to the previous discussion, these parameters are, for each temperature, the zero field (extrapolated) superfluid density $n_{s0}(T)$ and the upper critical field $H_{c2}(T)$. We will extract these values from microwave data and compare them with the values that are obtained from independent measurements. The values of n_{s0} and H_{c2} for each temperature can be obtained through a self-consistent procedure. As a first step, we notice that, if the value of $\nu_s(B,T)$ is known at any fixed temperature and field, $r_1(\nu,B,T)$ and $r_2(\nu,B,T)$ can be obtained from the measured ρ_1/ρ_n and ρ_2/ρ_n by inverting Eqs. (2). Although the frequency, temperature, and field dependence of r_1 and r_2 are not known *a priori*, the high frequency limit of r_1 is known: in fact, as discussed in Sec. II, at high enough frequency $R[\rho_v] \to \rho_{ff}$ so that, assuming the validity of the Bardeen Stephen expressions for the flux flow resistivity, one should have $r_1 \to b$ at large ν. We then choose a given temperature T_0 and calculate, for any value of H, a tentative value of ν_s through Eq. (4), using for n_s the value that can be obtained through Eq. (5) by fixing the values of $n_{s0}(T_0)$ and $H_{c2}(T_0)$. We then obtain for all fields $r_1(\nu,B,T_0)$ inverting Eqs. (2) and we check that they approach a constant value at high frequency. The values of $n_{s0}(T_0)$ and $H_{c2}(T_0)$ are then changed until, for all fields, the high frequency value for r_1 is equal to $b = H/H_{c2}(T_0)$.

In Fig. 4 we report the behavior of $n_{s0}(T)$, normalized to the lowest temperature value $n_{s0}(T=5\ \mathrm{K})$. Since $n_{s0} = K n_{s,\sigma}(B=0,T)$, this behavior should be compared with the temperature variation of $n_{s,\sigma}(B=0,T)$, as obtained in an independent way. We then calculate $n_{s,\sigma}(B=0,T)$ using the expressions of the BCS theory,[7] and the values of the gap

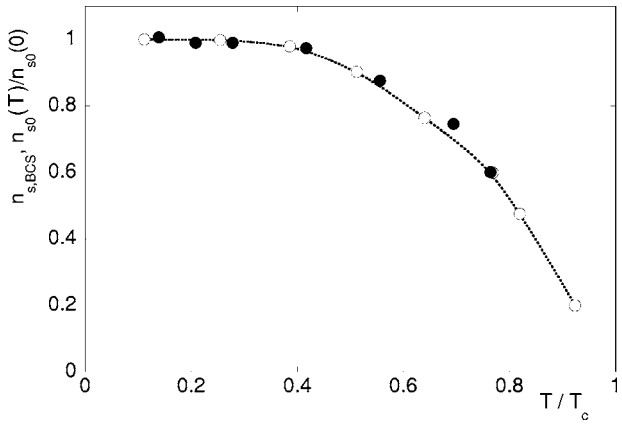

FIG. 4. The behavior of the obtained $n_{s0}(T)$ normalized to the low temperature value (full circles) together with the BCS calculation (open circles, see text). Dashed line is a guide for the eye.

$\Delta_\sigma(T)$ measured by point contact spectroscopy.[26] The agreement between our determination and the theoretical predictions is excellent and gives a strong support to the consistency of the analysis performed in this paper.

We also notice that if one further assumes that $n_{s,\sigma}(B=0,T=0)=1$, one may obtain the value of the prefactor CK, which is proportional to the ratio $\rho_n/\lambda_{0,\sigma}^2$. In this way, using the value of ρ_n that can be obtained through the dc measurement on our sample ($\rho_n = 5\mu\Omega\,\mathrm{cm}$), we obtain $\lambda_{0,\sigma} = 370$ nm. This value should be considered as an order of magnitude estimation, due to the approximations used through the analysis.

On the other hand, in Fig. 5 we report the upper critical field H_{c2} as obtained from our self-consistent procedure (full circles) and the upper critical field obtained independently from the dc measurements (open circles). Again, the agreement is excellent, further confirming the consistency of the underlying model. This is an important result of this paper: it is worthwhile to stress that previous analyses have never been able to describe the microwave data using the same

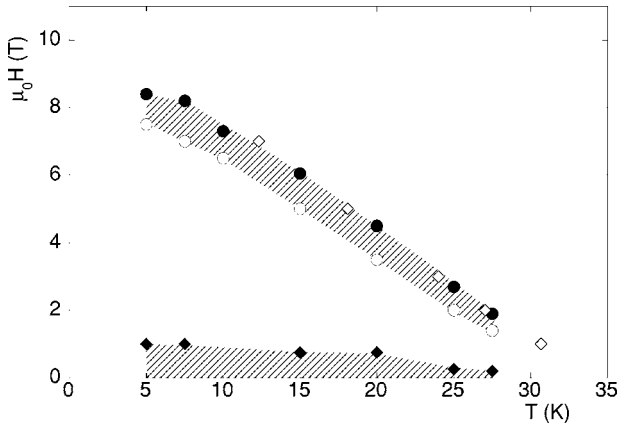

FIG. 5. The values of H_{c2} (full circles) as obtained from the self-consistent procedure described in the text. Values of H_1 (full diamonds) and H_2 (open diamonds) and the behavior of $H_{c2,\perp}^{dc}(T)$ as obtained from the *dc* measurements (open circles)are also reported. The dashed regions have the same meaning as in Fig. 1.

parameters obtained from low frequency measurements. In particular, the upper critical field was found to be field dependent[20] or anomalous field dependencies for the vortex viscosity were invoked.[5]

C. Vortex motion parameters

As a last step, we extract from our data the temperature and field dependence of the characteristic vortex frequency ν_0, in order to check the validity of the assumption $\nu_0 < 15$ GHz used in the discussion of Fig. 3 and to get information on the pinning phenomena in our film. To this end, we notice that Eqs. (2) can be inverted getting

$$\frac{\mathrm{Re}[\rho_v]}{\rho_n} = r_1 = \frac{\rho_1}{\rho_n} - \frac{\nu}{\nu_s}\frac{\rho_2}{\rho_n},$$

$$\frac{\mathrm{Im}[\rho_v]}{\rho_n} = r_2 - \frac{\rho_{nf}}{\rho_n}\frac{\nu}{\nu_s} = \frac{\rho_2}{\rho_n} + \frac{\nu}{\nu_s}\frac{\rho_1}{\rho_n} - \frac{\rho_{nf}}{\rho_n}\frac{\nu}{\nu_s}.$$

Using the values of ν_s and ρ_{nf}/ρ_n obtained previously, it is then possible to extract from our data the curves $\mathrm{Re}[\rho_v]/\rho_n(\nu)$ and $\mathrm{Im}[\rho_v]/\rho_n(\nu)$ describing the resistivity due to the vortex motion alone for any value of H and T. We may then compare the resistivity due to vortex motion to some specific expression for ρ_v as a function of ν, containing the parameter ν_0. We make use of the theory developed by Coffey and Clem,[11] which takes into account both creep and pinning for vortices. Within that theory, the real and imaginary parts of ρ_v are given by

$$\frac{\mathrm{Re}[\rho_v]}{\rho_n} = \frac{\rho_{ff}}{\rho_n}\frac{\epsilon + (\nu/\nu_0)^2}{1 + (\nu/\nu_0)^2},$$

$$\frac{\mathrm{Im}[\rho_v]}{\rho_n} = \frac{\rho_{ff}}{\rho_n}\frac{1-\epsilon}{1 + (\nu/\nu_0)^2}\frac{\nu}{\nu_0}, \tag{6}$$

where ρ_{ff} is the free flow value of the resistivity, which is given by $\rho_n B/B_{c2}$, and ϵ is a factor accounting for possible creep effects. We fitted all the curves $\mathrm{Re}[\rho_v]/\rho_n(\nu)$, $\mathrm{Im}[\rho_v]/\rho_n(\nu)$ at any given temperature and field, using as fitting parameters the two values ϵ and ν_0 ($\rho_{ff}/\rho_n = b$ is determined by the value of H_{c2} obtained previously). A typical result of the fitting procedure for $T=15$ K and $\mu_0 H = 3$ T is reported in Fig. 6 (solid lines). The obtained behavior of ν_0 is reported in the inset of Fig. 6 for various temperatures, as a function of the reduced field b. As can be seen, ν_0 never exceeds 10 GHz, for any temperature and field. Moreover, it results to be strongly field dependent, in agreement with previous findings,[4] suggesting a collective nature of the pinning forces in this material. This conclusion is also supported by the scaling, at low temperatures, of all curves $\nu_0(b)$. A detailed analysis of the vortex contribution to the microwave resistivity is left for future studies.

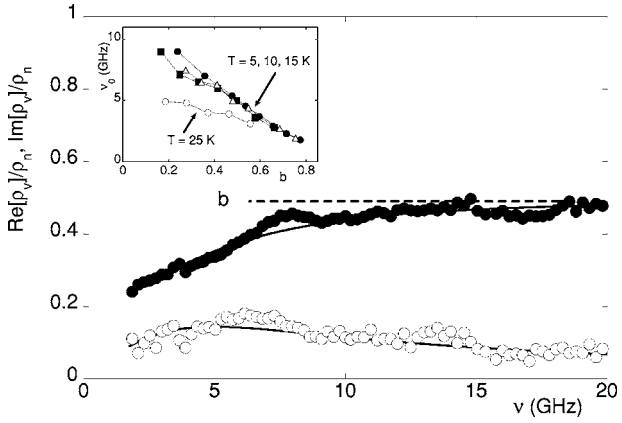

FIG. 6. Main panel: measured $\mathrm{Re}[\rho_v]/\rho_n = r_1$ and $\mathrm{Im}[\rho_v]/\rho_n = r_2 - (\rho_{nf}/\rho_n)(\nu/\nu_s)$ at $T=15$ K and $\mu_0 H = 3$ T. Solid lines are the fits through Eq. (6). Fitting parameters are $\epsilon = 0.42$ and $\nu_0 = 5$ GHz. The value of $b = H/H_{c2}$ (dashed line) is obtained through the self-consistent procedure used to determine n_{s0} and H_{c2} at this temperature (see text). Analogous results are obtained for all temperatures and fields. Inset: values of ν_0 at various temperatures, as a function of the reduced field $b = H/H_{c2}$.

V. CONCLUSIONS

We have presented in this paper complex resistivity microwave data in a large range of frequency. These wide band data allowed for the experimental determination of the region in the $\{H,T\}$ plane in which only one band contributes significantly to superconductivity. Within that region, the contributions to the resistivity coming from vortex motion and quasiparticles are identified and discussed. The σ-band superfluid density, the upper critical field, and the vortex characteristic frequency have been extracted and successfully compared to dc results and to previous findings.

ACKNOWLEDGMENTS

This work has been supported by the Istituto Nazionale di Fisica della Materia (INFM) under the national project PRA-U.M.B.R.A.

[1] See, e.g., special issue on MgB_2, edited by G. Crabtree, W. Kwok, P. C. Canfield, and S. L. Bud'ko, Physica (Amsterdam) **385C**, 1 (2003).

[2] F. Bouquet, R. A. Fisher, N. E. Phillips, D. G. Hinks, and J. D. Jorgensen, Phys. Rev. Lett. **87**, 047001 (2001); M. Iavarone, G. Karapetrov, A. E. Koshelev, W. K. Kwok, G. W. Crabtree, D. G. Hinks, W. N. Kang, Eun-Mi Choi, Hyun Jung Kim, Hyeong-Jin Kim, and S. I. Lee, *ibid.* **89**, 187002 (2002); R. S. Gonnelli, D. Daghero, G. A. Ummarino, V. A. Stepanov, J. Jun, S. M. Kazakov, and J. Karpinski, *ibid.* **89**, 247004 (2002).

[3] Mun-Seog Kim, John A. Skinta, Thomas R. Lemberger, W. N. Kang, Hyeong-Jin Kim, Eun-Mi Choi, and Sung-Ik Lee, Phys.

Rev. B **66**, 064511 (2002); B. B. Jin, N. Klein, W. N. Kang, Hyeong-Jin Kim, Eun-Mi Choi, Sung-Ik Lee, T. Dahm, and K. Maki, *ibid.* **66**, 104521 (2002).

[4] A. Dulčić, M. Požek, D. Paar, Eun-Mi Choi, Hyun-Jung Kim, W. N. Kang, and Sung-Ik Lee, Phys. Rev. B **67**, 020507(R) (2003).

[5] A. Shibata, M. Matsumoto, K. Izawa, Y. Matsuda, S. Lee, and S. Tajima, Phys. Rev. B **68**, 060501(R) (2003).

[6] E. Babaev, Phys. Rev. Lett. **89**, 067001 (2002).

[7] M. Tinkham, *Introduction to Superconductivity*, 2nd ed. (McGraw-Hill, New York, 1996).

[8] M. R. Eskildsen, M. Kugler, S. Tanaka, J. Jun, S. M. Kazakov, J. Karpinski, and Ø. Fischer, Phys. Rev. Lett. **89**, 187003 (2002).

[9] R. S. Gonnelli, D. Daghero, A. Calzolari, G. A. Ummarino, V. Dellarocca, V. A. Stepanov, J. Jun, S. M. Kazakov, and J. Karpinski, Phys. Rev. B **69**, 100504(R) (2004).

[10] R. Cubitt, M. R. Eskildsen, C. D. Dewhurst, J. Jun, S. M. Kazakov, and J. Karpinski, Phys. Rev. Lett. **91**, 047002 (2003).

[11] M. W. Coffey and J. R. Clem, Phys. Rev. Lett. **67**, 386 (1991).

[12] We note that at our frequencies ($\nu < 20$ GHz) σ_n is expected be real and independent on frequency.

[13] J. I. Gittleman and B. Rosenblum, Phys. Rev. Lett. **16**, 734 (1966).

[14] See, e.g., N. P. Ong and H. Wu, Phys. Rev. B **56**, 458 (1997); A. T. Dorsey, *ibid.* **43**, 7575 (1992); C. J. van der Beek, V. B. Geshkenbein, and V. M. Vinokur, *ibid.* **48**, 3393 (1993); E. B. Sonin, A. K. Tagantsev, and K. B. Traito, *ibid.* **46**, 5830 (1992); B. Plaçais, P. Mathieu, Y. Simon, E. B. Sonin, and K. B. Traito, *ibid.* **54**, 13083 (1996).

[15] V. Ferrando, S. Amoruso, E. Bellingeri, R. Bruzzese, P. Manfrinetti, D. Marré, R. Velotta, X. Wang, and C. Ferdeghini, Supercond. Sci. Technol. **16**, 241 (2003).

[16] V. Ferrando, P. Manfrinetti, D. Marré, M. Putti, I. Sheikin, C. Tarantini, and C. Ferdeghini, Phys. Rev. B **68**, 094517 (2003).

[17] This approximation holds until $\lambda > d/2$, see E. Silva, M. Lanucara, and R. Marcon, Supercond. Sci. Technol. **9**, 934 (1996).

[18] S. Sarti, C. Amabile, and E. Silva, cond-mat/0406313.

[19] S. Sarti, E. Silva, C. Amabile, R. Fastampa, and M. Giura, Physica C **404**, 330 (2004).

[20] A. Dulčić, D. Paar, M. Požek, G. V. M. Williams, S. Krämer, C. U. Jung, Min-Seok Park, and Sung-Ik Lee, Phys. Rev. B **66**, 014505 (2002).

[21] A. E. Koshelev and A. A. Golubov, Phys. Rev. Lett. **90**, 177002 (2003).

[22] I. I. Mazin, O. K. Andersen, O. Jepsen, O. V. Dolgov, J. Kortus, A. A. Golubov, A. B. Kuz'menko, and D. van der Marel, Phys. Rev. Lett. **89**, 107002 (2002).

[23] A. Gurevich, Phys. Rev. B **67**, 184515 (2003).

[24] V. Ferrando, C. Tarantini, P. Manfrinetti, D. Marré, M. Putti, A. Tumino, and C. Ferdeghini, in *Proceedings of 6th European Conference on Applied Superconductivity*, edited by A. Andreone, G. P. Pepe, R. Cristiano and G. Masullo (Institute of Physics, Sorrento, 2003), p. 1263.

[25] P. Seneor, C.-T. Chen, N.-C. Yeh, R. P. Vasquez, L. D. Bell, C. U. Jung, Min-Seok Park, Heon-Jung Kim, W. N. Kang, and Sung-Ik Lee, Phys. Rev. B **65**, 012505 (2001); J. W. Quilty, S. Lee, A. Yamamoto, and S. Tajima, Phys. Rev. Lett. **88**, 087001 (2002).

[26] P. Szabó, P. Samuely, J. Kacmarcik, T. Klein, J. Marcus, D. Fruchart, S. Miraglia, C. Marcenat, and A. G. M. Jansen, Phys. Rev. Lett. **87**, 137005 (2001).